Brazilian Journal
of Chemical
Engineering

ISSN 0104-6632
Printed in Brazil
www.abeq.org.br/bjche

Vol. 29, No. 01, pp. 121 - 133, January - March, 2012

PREPARATION AND PROPERTIES OF NANOPHASE (Ce, Zr, Pr)O_2-DOPED ALUMINA COATING ON CORDIERITE CERAMIC HONEYCOMB FOR THREE-WAY CATALYSTS

Jiuying Tian* and Jusheng Lu

School of Chemistry & Chemical Engineering, Jiangsu Key Laboratory of Green Synthetic Chemistry for Functional Materials, Phone: +86 516 83403165, Fax: +86 516 83536977, Xuzhou Normal University, Xuzhou 221116, P.R. China.
E-mail: jiuyingtian@163.com

(Submitted: January 4, 2011 ; Revised: April 16, 2011 ; Accepted: September 7, 2011)

Abstract - Nanophase (Ce, Zr, Pr)O_2-doped alumina coatings were prepared by impregnating the cordierite ceramic honeycomb in the sol or in the slurry of already calcined powder, respectively. The effects of preparation methods on the crystal phase, texture, oxygen storage capacity (OSC), reducibility, surface morphology and thermal stability of coatings were investigated by X-ray diffraction (XRD), the Brunauer Emmet Teller (BET) method, the oxygen pulsing technique, H_2-temperature-programmed reduction (H_2-TPR) and scanning electron microscopy (SEM). These nanophase (Ce, Zr, Pr)O_2-doped alumina coatings were used as supports to prepare Pd-only three-way catalysts, and evaluated with respect to catalytic activities. The results indicate that the nanophase (Ce, Zr, Pr)O_2-doped alumina coatings prepared by the two methods have high thermal stability. However, the coating derived from the sol shows better crystalline structure, texture, reducibility and oxygen storage capacity than the coating derived from the slurry. SEM observation shows that the morphology of the coating derived from the sol is uniform and smooth. The Pd-only catalyst derived from the sol exhibits high three-way catalytic activity at low temperature and thermal stability, suggesting a great potential for applications.
Keywords: Nanophase (Ce, Zr, Pr)O_2; Coating; Preparation; Properties; Three-way catalyst.

INTRODUCTION

Three-way catalysts (TWC) for automobile exhaust purification are comprised mainly of three parts: a cordierite honeycomb substrate, an activity coating and a noble metal (Pt, Rh, Pd) activity element (Muraki and Geng, 2000; Gonzalez-Velasco *et al*., 2001). The cordierite ceramic substrate (2MgO • $2Al_2O_3$ • $5SiO_2$) has high mechanical strength, a small pressure drop and a low thermal expansion coefficient (Zotin *et al*., 2005), but the specific surface area of the cordierite ceramic honeycomb is small ($<1 m^2.g^{-1}$). In order to improve the catalytic activity, a coating material of high specific surface area should be deposited on the surface layer of the cordierite ceramic honeycomb (Hirohumi *et al*., 2001; Stary *et al*., 2006). γ-Alumina is a coating material that is currently being used to expand the specific surface area (Yue *et al*., 2005; Aguila *et al*., 2008). However, the surface area loss becomes pronounced above 1000°C as the γ-alumina phase is converted to the θ-phase and finally to the α-form (Kucharczyk *et al*., 2004). Studies have shown that a stabilizer, such as CeO_2, La_2O_3 or Y_2O_3, can delay the phase transition temperature of γ-alumina and reduce the loss of specific surface area (Agrafiotis *et*

*To whom correspondence should be addressed

al., 2000; Mokhnachuk *et al*., 2007; Yassir and VanMao, 2007).

CeO_2 has been widely studied in recent years because of its potential usefulness for catalytic applications (Kaspar and Fornasiero, 2003; Kakuta *et al*., 2006). It is well known that CeO_2 can affect: (i) thermal and structure stability of the catalyst supports (Piras *et al*., 2000); (ii) dispersion of supported metal (Montoya *et al*., 2000); (iii) oxidation and reduction of noble metals (Bozo *et al*., 2001); (iv) storage and release of oxygen (Hadi and Yaacob, 2004), etc. Especially when the grain size of CeO_2 is nanometer, a large number of lattice defects such as oxygen vacancies are present, which provide the active sites of gas-solid catalytic reaction. The number of defects can be increased by partial substitution of the cerium atoms in the cerium oxide lattice with other metal atoms such as Zr, La, Nd or Pr. Because of these properties, CeO_2-based mixed oxides such as (Ce, Zr)O_2 and (Ce, Zr, M)O_2 (M= La, Y, Pr, Nd, etc.) are efficient oxygen storage materials, which can act as catalysts themselves and significantly reduce the need for noble metals (He *et al*., 2003; Fagg *et al*., 2006; Wu *et al*., 2007). Researchers have focused their attention on (Ce, Zr)O_2 or (Ce, Zr, M)O_2 doped alumina (Fernandez-Garcia *et al*., 2000; Damyanova *et al*., 2002; Wei *et al*., 2008; Morikawa *et al*., 2008; Morikawa *et al*., 2009; Zhu *et al*., 2010), which is a valid combination for environmental application catalysts, such as catalysts for removal of pollutants from auto-exhaust streams. When nanophase (Ce, Zr, M)O_2-doped alumina is deposited on cordierite ceramic honeycomb, the whole coating can be used for high-temperature catalytic applications.

At present, nanophase (Ce, Zr, M)O_2-doped alumina material is deposited on cordierite ceramic honeycomb by the dip coating method, which is an economical and simple method used in practice (Agrafiotis *et al*., 2002; Jiang *et al*., 2005; Chen *et al*., 2006; Guo *et al*., 2007; Tian *et al*., 2010). Active nanophase (Ce, Zr, M)O_2 powder can be effectively synthesized through liquid precursor solutions via wet chemistry methods. This nanophase (Ce, Zr, M)O_2 powder needs to be processed as slurries for impregnating the cordierite ceramic honeycomb. After subsequent calcination, this method leads to a coating layer deposited on the honeycomb walls. However, there are few reports of impregnating the honeycomb directly in the sol phase. In addition, (Ce, Zr)O_2 and (Ce, Zr, La)O_2 have been widely applied in TWC (Wu *et al*., 2004; Jiang *et al*., 2005; Guo *et al*., 2007; Chen *et al*., 2006), but relatively little attention has been paid to the nanophase (Ce, Zr, Pr)O_2 solid solution. Here we report a novel sol-gel method for preparing a nanophase (Ce, Zr, Pr)O_2-doped alumina coating on cordierite ceramic honeycomb.

In the previous works, the authors prepared the nanophase (Ce, Zr, Pr)O_2 solid solution by co-precipitation (Tian *et al*., 2006) and studied the preparation conditions of a pure alumina coating on cordierite ceramic honeycomb, using boehmite as the raw material (Tian *et al*., 2010). In the present work, we prepared (Ce, Zr, Pr)O_2-doped alumina coatings by impregnating the cordierite ceramic honeycomb in the sol and in the slurry of already calcined powder, respectively. The effects of preparation methods on the crystalline structure, texture, reducibility, oxygen storage capacity and thermal stability of coatings were studied. These (Ce, Zr, Pr)O_2-doped alumina coatings were used as supports to prepare Pd-only catalysts so that the whole support/catalyst system can be evaluated under operating conditions simulating automotive exhaust gases. The aim of this work was to obtain an uniform nanophase (Ce, Zr, Pr)O_2-doped alumina coating support with high catalytic activity and thermal stability.

EXPERIMENTAL

Preparation of Supports

The slurry was prepared as follows: the nanophase (Ce, Zr, Pr)O_2 powder was prepared by the co-precipitation method described in the previous work (Tian *et al*., 2006). Then this (Ce, Zr, Pr)O_2 nano-oxide powder was mixed with a boehmite sol, which was prepared by a technique similar to the literature (Tian *et al*., 2010). After stirring, the slurry was obtained for impregnating honeycombs.

Another method for the coating of cordierite ceramic honeycomb is the sol-gel method. First, the (Ce, Zr, Pr)O_2 precursor sol was prepared as follows: $Ce(NO_3)_3{\cdot}6H_2O$, $Zr(NO_3)_4{\cdot}5H_2O$, $Pr(NO_3)_3{\cdot}6H_2O$ and citric acid were dissolved in de-ionized water. Its pH value was adjusted with aqueous $NH_3{\cdot}H_2O$ solution. This mixture solution was heated at 70°C in a water bath and constantly stirred until a stable sol was obtained. Then this (Ce, Zr, Pr)O_2 precursor sol was mixed with the above-mentioned boehmite sol to form a final sol, which was used to impregnate the cordierite ceramic honeycomb.

For the final sol and the slurry, the relative molar ratios of each constitute were (Ce, Zr, Pr)O_2/Al_2O_3 = 1:3, Ce/Zr/Pr = 12:7:1.

A commercial honeycomb cordierite cast (Corning Corporation, 400 cells per square inch) was

cut into cylinder samples (10 mm diameter × 25 mm length) and employed for the impregnation experiment. The cordierite specimens were immersed in the sol or slurry prepared by the above-mentioned methods. The loaded specimens were withdrawn and the excess slurry was removed by blowing air through the honeycomb channels. Subsequently, the coated honeycombs were dried at 120°C for 2 h in air and calcined at 550°C for 5 h in air (heating rate 10°C min^{-1}), so that the fresh (Ce, Zr, Pr)O_2-doped alumina coatings on cordierite ceramic honeycombs were formed. The aged samples were obtained by aging the fresh samples at 1000°C for 3 h in air (heating rate 10°C min^{-1}). The (Ce, Zr, Pr)O_2-doped alumina coatings prepared by impregnating the honeycomb in the sol and in the slurry were abbreviated as CZPA-S and CZPA-P, respectively.

Preparation of Catalysts

Catalysts were prepared by the classical post-impregnation method. The cordierite ceramic honeycombs loaded with the (Ce, Zr, Pr)O_2-doped alumina coatings were subsequently post-impregnated with H_2PdCl_4 aqueous solutions, whose volumes were adjusted for complete absorption by the coating. The Pd loadings were 0.8 g L^{-1}. After the post-impregnation, the cordierite catalysts were dried at 120°C for 3 h in air and calcined at 550°C for 5 h in air (heating rate 10°C min^{-1}) to obtain the fresh catalysts. The aged catalysts were obtained by thermal treatment of fresh catalysts at 1000°C for 3 h in air (heating rate 10°C min^{-1}). The catalyst prepared from CZPA-S was labeled Pd/CZPA-S, while that prepared from CZPA-P was labeled Pd/CZPA-P.

Characterization of Supports and Catalysts

Powder X-ray diffraction (XRD) patterns were collected on a Rigaku D/max-III B powder diffraction instrument, using CuKα radiation, operated at 35 kV and 30 mA. The intensity data were collected in a 2θ range from 10° to 70°.

Surface area analysis was carried out at liquid N_2 temperature with the Brunauer-Emmet-Teller (BET) method using ASAP2010 micromeritics.

The surface morphology was examined with a Hitachi S-3400N scanning electron microscope, operated at an accelerated voltage of 20KV. Prior to SEM analysis, the cordierite honeycomb loaded with (Ce, Zr, Pr)O_2-doped alumina coating was cut along the channel, so that the coating inside the channel was exposed. Before examination, this coating was covered with a thin layer of gold by sputtering, which was used as an electrically conductive film to prevent charging.

Total oxygen storage capacity (OSC) was measured by gas chromatography in flowing N_2 (30 ml min^{-1}) at 200°C. Prior to the experiment, the sample (200 mg) was reduced at the appropriate temperature (500°C) for 30 min under a H_2 flow (40 ml min^{-1}). After reduction, the sample was cooled to 200°C under N_2 flow (30 mL min^{-1}). Then a given amount of oxygen (0.15 ml) was pulsed every 5 min until the intensity of the peak reached a constant value, which means that no additional oxygen consumption could be detected by the thermal conductivity detector (TCD).

H_2-temperature-programmed reduction (H_2-TPR) experiments were performed in a quartz tubular microreactor. The sample (200 mg) was placed in a quartz reactor. A thermocouple was located in the middle of the reactor, the reactor was placed in a tubular furnace, and a temperature-programmed controller was used to adjust the reactor temperature. In order to remove the moisture produced during H_2-TPR, the outlet of the quartz tubular reactor was connected to a glass column packed with 5A molecular sieve. The sample was first pretreated at 400°C for 1 h under N_2 flow (30 ml min^{-1}), cooled to room temperature, and swept with H_2-N_2 (H_2:N_2 5:95) at a rate of 30 ml min^{-1} until the base line on the recorder remained unchanged. Finally, the sample was heated at the rate of 10°C min^{-1} under flowing H_2-N_2 (H_2:N_2 5:95, flow rate 30 ml min^{-1}) from room temperature to 900°C. H_2 consumption during reduction was detected by a thermal conductivity detector (TCD).

Catalytic Tests of Catalysts

The three-way catalytic activity was evaluated in a conventional fixed-bed flow quartz micro-reactor by passing a gas mixture similar to exhaust from a gasoline engine. The gases were regulated using mass-flow controllers. The catalyst was held in a quartz tube by packing quartz wool at both ends of the catalyst bed. The quartz tube was placed in a tubular furnace and the temperature of the catalyst was controlled by a temperature-programmed controller. The simulated exhaust containing a mixture of CO (0.7%), C_3H_8 (0.05%), NO (0.05%), CO_2 (10%), O_2 (0.6%) and N_2 (balance) was fed to the reactor at a gas space velocity of 30,000h^{-1}. The concentrations of CO, NO and C_3H_8 were analyzed online by a FGA-4015 analyzer before and after

simulated gas passing through the micro-reactor. Conversion data were measured from 50 to 400°C with a rate of 5°C min^{-1}. The curves of the relationship between conversion and temperature were obtained. The catalytic activity of catalyst was expressed as the light-off temperature ($T_{50\%}$), at which the target reactant (CO, NO or C_3H_8) had been converted by 50%.

RESULTS AND DISCUSSION

XRD

X-ray diffraction patterns of the supports and the Pd-supported samples are shown in Fig. 1. For CZPA-S and CZPA-P (Fig. 1a), a single fluorite-type phase of (Ce, Zr, Pr)O_2 solid solution and the γ-alumina phase are observed in all fresh samples. The diffraction peaks at 2θ = 28.8˚, 33.3˚, 47.5˚, 56.6˚, which correspond to the (111), (200), (220), (311) crystal planes for the cubic fluorite structure, are ascribed to a single phase of uniform (Ce, Zr, Pr)O_2 solid solution (Tian *et al*., 2006). The characteristic diffraction peaks of γ-alumina are of low intensity and the most intense peak is around 2θ = 67.3˚. Samples did not show any clear diffraction peaks of cerium aluminate ($CeAlO_3$) (2θ = 23.5, 33.5, 41.4 and 60˚) (Damyanova *et al*., 2002) and praseodymium aluminate ($PrAlO_3$) (2θ = 23.3, 33.9, 42.1 and 48.5˚) (Pawlak *et al*., 2005). This indicates that the (Ce, Zr, Pr)O_2 solid solution does not combine with alumina to form the new species. After thermal treatment at 1000°C, the intensities of the diffraction peaks of the (Ce, Zr, Pr)O_2 solid solution increase and the line-broadenings decrease. No phase other than alumina and (Ce, Zr, Pr)O_2 was observed in the XRD profiles. The supports CZPA-S and CZPA-P show γ- and δ-alumina, respectively. We did not detect any α-alumina, although pure γ-alumina should be converted to α-alumina at 1000°C (Kucharczyk *et al*., 2004), indicating that the presence of (Ce, Zr, Pr)O_2 obviously improved the thermal stability of alumina, as already reported in the literature (Monte *et al*, 2000; Yue *et al*, 2005; Wang *et al*., 2010). It also indicates that the (Ce, Zr, Pr)O_2-doped alumina coatings prepared by the two methods have high thermal stability. After thermal treatment, the CZPA-S still shows γ-alumina; however, CZPA-P converted to δ-alumina, indicating that the thermal stability of CZPA-S is higher than that of CZPA-P.

For fresh and aged Pd/CZPA-S and Pd/CZPA-P (Fig. 1b), the characteristic peaks of metallic Pd (2θ = 40.4 and 41.9°) cannot be distinguished from the main peaks of the support. This suggests that Pd particles are well dispersed on the supports, which makes them hard to be detected by XRD. The structures of the supports remain essentially unchanged and alumina and (Ce, Zr, Pr)O_2 solid solution phase are detected, which is consistent with results reported in the literature (Zhao *et al*., 2009; Yue *et al*., 2005; Cai *et al*, 2008).

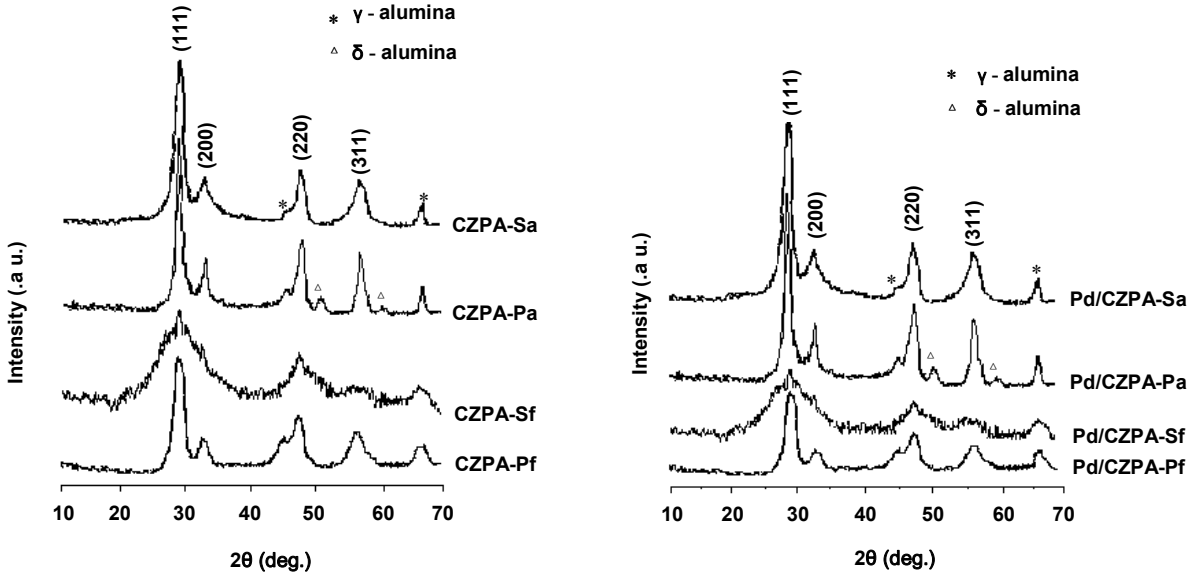

Figure 1: X-ray diffraction patterns of: (a) supports and (b) Pd-supported samples (f-fresh samples, a-aged samples).

The crystallite sizes of the (Ce, Zr, Pr)O_2 solid solution were calculated by Scherrer's equation from the full-width at half maximum of the XRD profiles. The crystallite sizes of (Ce, Zr, Pr)O_2 are 2.3 nm and 4.3 nm for fresh CZPA-S and CZPA-P, respectively. After thermal treatment at high temperature, the crystallite sizes of (Ce, Zr, Pr)O_2 are increased to 13.1 nm for CZPA-P, whereas it only increased to 6.8 nm for CZPA-S. The results also suggest that the thermal stability of CZPA-S is higher than that of CZPA-P. The crystallite size is still nanometer scale after thermal treatment. Furthermore, there is no solid phase reaction between alumina and the (Ce, Zr, Pr)O_2 solid solution at high temperature, i.e., they still exist as single phases. It is plausible that alumina and (Ce, Zr, Pr)O_2 are well dispersed at the nanometer level, which could serve as a diffusion barrier to each other (Morikawa *et al*., 2008) and inhibit mutual particle growth, consequently resulting in samples with good stability of crystal particles at high temperature. The results indicate that the nanophase (Ce, Zr, Pr)O_2 doped into alumina can stabilize and improve the thermal stability compared with pure alumina, which is consistent with the results of the XRD patterns.

For Pd-supported samples, the crystallite sizes are 3.6 nm and 5.1 nm for fresh Pd/CZPA-S and Pd/CZPA-P, respectively. The crystallite sizes are 8.0 nm and 12.6 nm for aged Pd/CZPA-S and Pd/CZPA-P, respectively. The crystallite sizes of Pd/CZPA-S are smaller than those of Pd/CZPA-P before and after aging. Moreover, the crystallite size increase of Pd/CZPA-P is greater than that of Pd/CZPA-S, indicating that Pd/CZPA-S has higher thermal stability than Pd/CZPA-P. This result shows that the thermal stability of the support is relevant for the properties of the catalyst. The catalyst usually works at temperature higher than 600°C. Strong thermal sintering of the support or the catalyst may cause a serious decrease of catalytic activity. The supports with high thermal stability could resist the sintering of catalyst after thermal treatment. The stability of CZPA-S is more suitable for the support of TWC.

Texture and Oxygen Storage Capacity

The specific surface area, pore volume, pore diameter and oxygen storage capacity of two supports before and after aging are shown in Table 1. The specific surface areas are 152.6 m^2/g for fresh CZPA-S and 130.2 m^2/g for fresh CZPA-P. After thermal treatment, the specific surface areas of CZPA-S and CZPA-P are still 123.4 m^2/g and 96.3 m^2/g, respectively. The specific surface area of CZPA-S is larger than that of CZPA-P before and after aging. Moreover, the decrease of the specific surface area of CZPA-S is smaller than that of CZPA-P, indicating that CZPA-S has higher thermal stability than CZPA-P. The pore volume of fresh CZPA-S is 0.47 ml/g, which is slightly larger than that of fresh CZPA-P (0.42 ml/g). The average pore sizes of fresh CZPA-S and CZPA-P supports are 4.02 and 4.81 nm, respectively. After thermal treatment, the average pore size increases to 4.38 nm for CZPA-S and 5.52 nm for CZPA-P. The increase of the average pore size of CZPA-S is 9.0%, while the average pore size increases by 14.8%, indicating that CZPA-S has higher thermal stability than CZPA-P.

The oxygen storage capacity of fresh CZPA-S is 628.2 μmol/g and decreases to 563.7 μmol/g (10.3%) after aging, while that of CZPA-P decreases from 516.3 μmol/g to 443.1 μmol/g (14.2%). The oxygen storage capacity and thermal stability of CZPA-S are higher than those of CZPA-P. It has been reported that the deactivation of TWC results mainly from the decrease of the oxygen storage amount (Kaspar and Fornasiero, 2003). Moreover, in heterogeneous catalysis, the surface of the support could provide the necessary active sites for catalytic reactions. The smaller the support particles are, the more surface sites of the support there are, and thus the higher the catalytic activity of the catalyst. Therefore, the good oxygen storage capacity and texture of the supports play an important role in the catalytic performance of the catalyst. Since CZPA-S exhibits better texture and oxygen storage capacity, it should be more suitable for the support of TWC, which is consistent with the XRD results.

Table 1: Textures and oxygen storage capacity (OSC) of samples

Sample		Specific surface area (m^2/g)	Pore volume (ml/g)	Pore diameter (nm)	OSC (μmol/g)
CZPA-S	fresh	152.6	0.47	4.02	628.2
	aged	123.4	0.42	4.38	563.7
CZPA-P	fresh	130.2	0.42	4.81	516.3
	aged	96.3	0.35	5.52	443.1

H_2-TPR

The reducibility of the support and supported catalyst is an important factor influencing its catalytic performance. H_2-TPR is a common technique to investigate the reducibility of samples (Salasc *et al*., 2002; Lin *et al*., 2004; Yeste *et al*. 2009). The H_2-TPR profiles of supports and Pd-supported catalysts are shown in Fig. 2. From Fig. 2a, the reduction profiles of CZPA-S are obviously different from those of CZPA-P, indicating that the preparation methods significantly affect the reduction behavior of the samples. The fresh CZPA-S shows a single main peak at 570°C, with broad shoulders at 440 and 533°C. However, for fresh CZPA-P, two reduction peaks at 619 and 782°C are observed, respectively. According to the literature (Silva *et al*., 2008), pure alumina commonly has no hydrogen consumption in the TPR profile. The pure ceria exhibits two reduction peaks at approximately 500 and 830°C, which are associated with the reduction of surface and bulk, respectively (Yao *et al*., 1984). The low-temperature reducibility (below 600°C) of the fresh CZPA-S sample is typically characterized by the presence of more than one overlapping peak. Moreover, no high temperature reduction peak is found. We suggest that there are two possible reasons: (i) according to the XRD and BET results, fresh CZPA-S presents a smaller crystal size and a higher surface area than fresh CZPA-P, which makes the surface Ce^{4+} easier to reduced at a lower temperature. (ii) the mobility of bulk oxygen in fresh CZPA-S is greatly enhanced due to the doping with ZrO_2, Pr_6O_{11} and Al_2O_3 (Wu *et al*., 2007; Morikawa *et al*., 2009). The bulk oxygen can move to the surface or subsurface more easily during the reduction process. Therefore, the multimodal shape of fresh CZAP-S can be attributed to the reduction of surface and subsurface Ce^{4+} of the mixed oxide crystallites and a successive reduction in the bulk (Wu *et al*., 2005; Vidal *et al*., 2000; Fally *et al*., 2000; Zhang *et al*., 2009). For fresh CZPA-P, the presence of two reduction peaks at 619 and 782°C indicates that there are at least two types of Ce^{4+} located in different chemical environments. The reduction peak at 619°C could be assigned to the reduction of surface Ce^{4+}, whereas the peak at 782°C could be assigned to the reduction of bulk Ce^{4+} (He *et al*., 2003; Kim *et al*., 2007; Kim *et al*., 2009; Thammachart *et al*., 2001). The temperature of bulk reduction of fresh CZPA-P is lower than that of pure CeO_2 (Boaro *et al*., 2003) due to the increased mobility of bulk oxygen in fresh CZPA-P. After thermal aging, the reduction peaks in the TPR experiment with CZPA-S sample shifts slightly towards lower temperature. A main peak at 562°C with a shoulder at 409°C is observed. Furthermore, the low temperature shoulder at 440°C disappears. This may be related to the loss of surface area and increase of crystal size, which decrease the surface activity of the sample. For the aged CZPA-P, a decrease of the maximum reduction temperature took place, which leads to a merging of TPR peaks. A single peak at 618°C is observed. It indicates that the promotion of the reducibility at low temperature could be induced by solid solution sintering at high temperature (Balducci *et al*., 1995; Otsuka-Yao-Matsuo *et al*., 1998; Fornasiero *et al*., 1999; Kaspar *et al*., 2003a; Wei *et al*., 2008). The results also indicate that CZPA-S and CZPA-P supports have excellent resistance to aging.

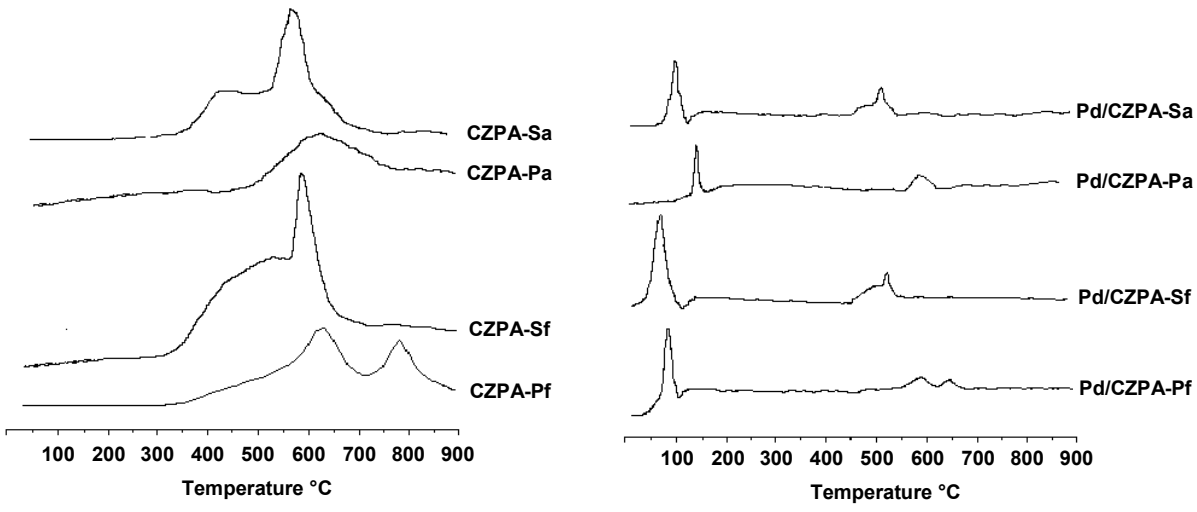

(a) (b)

Figure 2: H_2-TPR profiles of: (a) supports and (b) Pd-supported samples (f-fresh samples, a-aged samples).

Compared with CZPA-P, the reduction of CZPA-S begins at a lower temperature and its reduction peak area is larger, indicating that the CZPA-S support possesses the better reduction capacity. This result is mainly related to the smaller crystallite particle size and higher specific surface area of CZPA-S. It has been found (Perrichon *et al*., 1994) that the reduction of ceria occurs first on the surface and then progressively affects the bulk. It is said that the initial progress of reduction is highly sensitive to the surface area of the sample (Pan *et al*., 2009). Therefore, the specific surface area of CZPA-S is higher, which is more beneficial to the reduction of CZPA-S.

The reducibility of Pd-supported catalysts is an important factor influencing their catalytic activity. H_2-TPR profiles of fresh and aged Pd-supported catalysts are shown in Fig. 2b. From Fig. 2b, it can be seen that the H_2-TPR profiles of all catalysts exhibit one new reduction peak at low temperature compared to those of the pure supports. According to the literature (Luo *et al*., 1999; Barrera *et al*., 2001; Sun *et al*., 2004; Yue *et al*., 2005; Barrera *et al*., 2005; Yue *et al*., 2006), the H_2-TPR profiles of Pd/Ce-Zr-O catalyst show that the PdO species are reduced at 60-90°C, Thus, for the fresh catalyst, the reduction peak below 100°C may reflect the consumption of hydrogen by the reduction of PdO. Kaspar *et al*. (Kaspar *et al*., 2003b) reported that the active phase of Pd three-way catalyst is PdO. The transformation from PdO to Pd determines the catalytic performance of the catalysts. The lower reduction temperature of PdO can give the higher catalyst activity. The reduction peak temperatures are 73 and 88°C for fresh Pd/CZPA-S and Pd/CZPA-P, respectively. Therefore, Pd/CZPA-S exhibits the better reduction capacity and catalytic activity. In addition, the reduction peaks above 400°C, ascribed to the reduction of surface and bulk Ce^{4+}, are still evident, but shift to lower temperature compared with those of pure supports, which can be attributed to Pd-promoted reduction of CeO_2 via spillover of hydrogen (Kaspar *et al*., 2003b; Hickey *et al*., 2001). After aging, the reduction peaks of PdO shift to higher temperature, indicating that the transformation from PdO to Pd became more difficult, which possibly resulted from sintering of the active components. Moreover, the intensity of the reduction peak in the low-temperature region is weakened for aged catalysts, implying that Pd was partly sintered after aging (Wang *et al*, 2008). The aged Pd/CZPA-S was reduced at a lower temperature than aged Pd/CZPA-P, and the change in reduction temperature of Pd/CZPA-S is smaller before and after aging. The results indicate that Pd/CZPA-S has a stronger reduction capacity and higher thermal stability than Pd/CZPA-P.

SEM

The top views of (Ce, Zr, Pr)O_2-doped alumina coatings on monolith channels prepared by the two methods are presented in Fig. 3, where the details of the coating microstructure can be distinguished. First of all, the coating morphology was observed at low magnification (×50). The surface of CZPA-S is smooth and evenly distributed. However, a large number of tiny particles were obviously distributed on the surface of CZPA-P. This indicates that the preparation methods directly affect the surface morphology of the coatings. In order to observe better the microstructure of the coating, the photograph was magnified (×2000). The surface morphology of CZPA-P shows that the particles are aggregated in different sizes and geometries, less uniformly distributed on the substrate. These particles are mainly formed by combination between (Ce, Zr, Pr)O_2 powder particles and boehmite sol. However, compared with CZPA-P, CZPA-S shows a smooth layer. The reason is probably that CZPA-S is prepared by impregnating the cordierite ceramic honeycomb in the homogeneous sol phase.

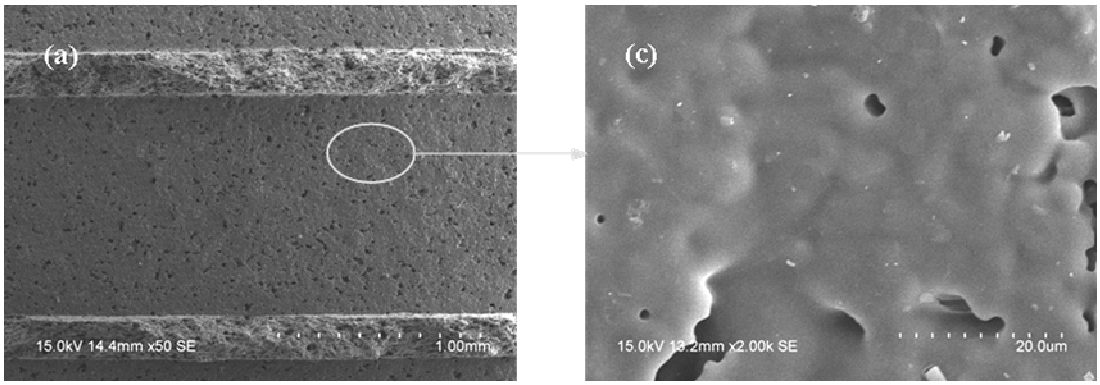

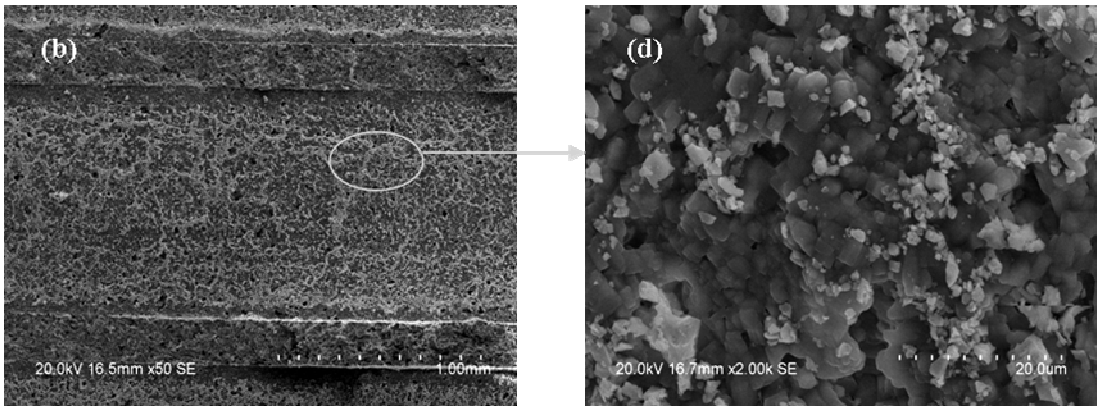

Figure 3: SEM photographs (top-view) of (Ce, Zr, Pr)O_2-doped alumina coating on honeycomb channels: (a) (c) CZPA-S, (b) (d) CZPA-P, (a) (b) low magnification, (c) (d) high magnification of the circular frame in images (a) and (b).

Catalytic Activity

In order to investigate the effect of coating supports on three-way catalysts, the catalytic activities of fresh and aged Pd-supported catalysts were evaluated. Fig. 4 presents the conversion of CO, C_3H_8 and NO over Pd/CZPA-S and Pd/CZPA-P catalysts. The light-off temperatures of the two catalysts are listed in Table 2. The light-off temperature of fresh Pd/CZPA-S catalyst is 180°C for CO, 195°C for C_3H_8, and 210°C for NO. The light-off temperature of fresh Pd/CZPA-P catalyst is 205°C for CO, 225°C for C_3H_8, and 234°C for NO. As reported by Cai *et al*. (2009), fresh Pd-only catalysts series supported on CeO_2-ZrO_2-BaO exhibit light-off temperatures in the range of 200-228°C for CO, 265-286°C for C_3H_8, 218-233°C for NO, which are higher than those of Pd/CZPA-S. However, they used a Pd-loading of 2 g/L, i.e. two times higher than that used in this work. The results show that Pd-only catalysts supported on a nanophase (Ce, Zr, Pr)O_2-doped alumina coating exhibit higher catalytic activity for CO and C_3H_8 oxidation and NO reduction. After thermal treatment, the light-off temperatures of Pd/CZPA-S and Pd/CZPA-P are 188°C and 220°C for CO, 217°C and 253°C for C_3H_8, 239°C and 278°C for NO, respectively. According to the report of Zhu *et al*. (1996), the conventional Pd/Al_2O_3 three-way catalyst contains a high quantity of precious metal (1.75 g/L), and the light-off temperature of aged catalyst is 287°C for the three components CO, C_3H_8 and NO, which is higher than those of the catalysts used in this work. It indicates that Pd/CZPA-S and Pd/CZPA-P have high thermal stability, which is consistent with the results of XRD and H_2-TPR. The conversion of NO is very important for TWC. Rh shows excellent activity to remove NO, but its high price and scarcity inhibit the development of TWC. In this work, the Pd-only catalysts supported on nanophase (Ce, Zr, Pr)O_2-doped alumina coatings show high activity of NO conversion. The light-off temperatures of fresh Pd/CZPA-S and Pd/CZPA-P are as low as 210 and 234°C, respectively, which are similar to the Pt/Rh TWC (Suopankia *et al*., 2005).

Based on the above analysis, CZPA-S and CZPA-P are suitable for use as supports of TWC owing to their high thermal stability and catalytic activity. However, compared with Pd/CZPA-P catalyst, the fresh and aged Pd/CZPA-S have lower light-off temperatures for CO, C_3H_8 and NO, which indicates that the Pd/CZPA-S catalyst exhibits high thermal stability and three-way catalytic activity. The catalytic activities are linked to the performance of the coating supports. Considering the results of support characterizations, we suggest that the main possible reasons are: (i) the CZPA-S support exhibits smaller crystallite size and larger specific surface area than CZPA-P, which could increase the dispersion of Pd species and provide more of the necessary activity sites for catalytic reactions; the catalyst would then have higher catalytic activity (Kim *et al*., 2000; Kolli *et al*., 2005). (ii) The CZPA-S support shows higher oxygen storage capacity and reduction capacity than CZPA-P, which can supply enough oxygen transport in the course of the reaction. (iii) The CZPA-S support has higher thermal stability than CZPA-P, which could resist the sintering of the catalyst. Therefore, the CZPA-S coating support derived from sol is more suitable as a support for TWC.

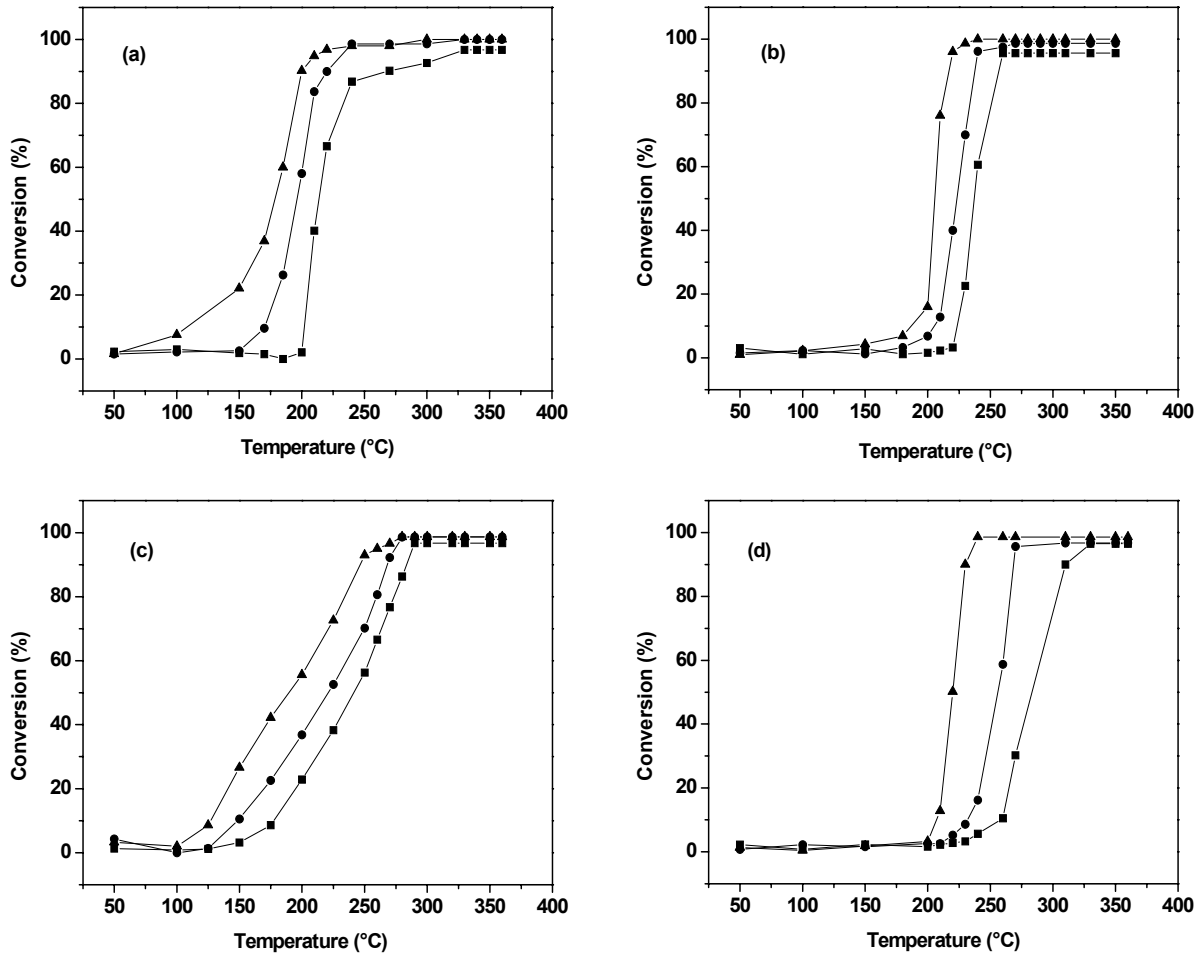

Figure 4: Conversion curves of CO (▲), C_3H_8 (●) and NO (■) as a function of temperature over Pd/CZPA-S and Pd/CZPA-P: (a) fresh Pd/CZPA-S, (b) fresh Pd/CZPA-P, (c) aged Pd/CZPA-S and (d) aged Pd/CZPA-P.

Table 2: Light-off light temperatures ($T_{50\%}$) of fresh and aged catalysts

Catalyst		Light-off temperature (°C)		
		CO	C_3H_8	NO
Pd/CZPA-S	fresh	180	195	210
	aged	188	217	239
Pd/CZPA-P	fresh	205	225	234
	aged	220	253	278

CONCLUSIONS

The present investigations have confirmed that the preparation methods have important effects on the crystal phase, texture, reducibility, oxygen storage capacity, surface morphology and thermal stability of the nanophase (Ce, Zr, Pr)O_2-doped alumina coating supports. In this work, the nanophase (Ce, Zr, Pr)O_2-doped alumina coatings prepared by the two methods have high thermal stability. The CZPA-S support demonstrates better texture, reducibility, oxygen storage capacity and thermal stability than the CZPA-P support. This is likely due to the greater interaction between the colloids at the sol stage. The Pd-only three-way catalyst derived from the sol shows low light-off temperature and high three-way catalytic activity, especially the excellent NO conversion and aging resistance.

ACKNOWLEDGEMENT

This study was supported financially by the Natural Science Foundation of Jiangsu Education Committee (07KJB150112), the Preliminary Research of the National Natural Science Foundation of China (08XLY05), and the Natural Science Foundation of Xuzhou Normal University (07XLA06).

REFERENCES

Agrafiotis, C., Tsetskou, A., Stournaras, C.-J., Julbe, A., Dalmazio, L., Guizard, C., Deposition of nanophase doped-ceria systems on ceramic honeycombs for automotive catalytic applications. Solid State Ionics, 136-137, 1301-1306 (2000).

Agrafiotis, C., Tsetsekou, A., Stournaras, C.-J., Julbe, A., Dalmazio, L., Guizard, C., Evaluation of sol-gel methods for the synthesis of doped-ceria environmental catalysis systems. Part I: preparation of coatings. Journal of European Ceramic Society, 22, No. 1, 15-25 (2002).

Aguila, G., Gracia, F., Araya, P., CuO and CeO_2 catalyst supported on Al_2O_3, ZrO_2, and SiO_2 in the oxidation of CO at low temperature. Applied Catalysis A: General, 343, No. 1-2, 16-24 (2008).

Balducci, G., Fornasiero, P., Di Monte, R., Kaspar, J., Meriani, S., Graziani, M., An unusual promotion of the redox behaviour of CeO_2-ZrO_2 solid solutions upon sintering at high temperatures. Catalysis Letters, 33, No. 1-2, 193-200 (1995).

Barrera, A., Viniegra M., Bosch, P., Lara, V.-H., Fuentes, S., Pd/Al_2O_3-La_2O_3 catalysts prepared by sol-gel: characterization and catalytic activity in the NO reduction by H_2. Applied Catalysis B: Environmental, 34, No. 2, 97-111 (2001).

Barrera, A., Viniegra, M., Fuentes, S., Diaz, G., The role of lanthana loading on the catalytic properties of Pd/Al_2O_3-La_2O_3 in the NO reduction with H_2. Applied Catalysis B: Environmental, 56, No. 4, 279-288 (2005).

Bozo, C., Guilhaume, N., Herrmann, J.-M., Role of the ceria–zirconia support in the reactivity of platinum and palladium catalysts for methane total oxidation under lean conditions. Journal of Catalysis, 203, No. 2, 393-406 (2001).

Boaro, M., Vicario, M., Leitenburg, C., Dolcetti, G., Trovarelli, A., The use of temperature programmed and dynamic/transient methods in catalysis characterization of ceria-base, model three-way catalysts. Catalysis Today, 77, No. 4, 407-417 (2003).

Cai, L., Zhao, M., Pi, Z., Gong M.-C., Chen Y.-Q., Preparation of Ce-Zr-La-Al2O3 and supported single palladium three-way catalyst. Chinese Journal of Catalysis, 29, No. 2, 108-112 (2008).

Cai, L., Chen, S.-H., Zhao, M., Gong, M.-C., Shi, Z.-H., Chen, Y.-Q., Pd supported three-way catalyst preparation of CeO_2-ZrO_2-BaO support and catalytic performance. Chinese Journal of Inorganic Chemistry, 25, No. 3, 474-479 (2009).

Chen, J.-J., Feng, C.-G., Shu, B.-C., Fan, J., Influence of different subsistence states of CeO_2-ZrO_2 mixed oxides in catalyst coating on catalytic properties. Journal of Rare Earths, 24, No. 1, 54-59 (2006).

Damyanova, S., Perez, C.-A., Schmal, M., Bueno, J.-M.-C., Characterization of ceria-coated alumina carrier. Applied Catalysis A: General, 234, No. 1-2, 271-282 (2002).

Fagg, D.-P., Frade, J.-R., Kharton, V.-V., Marozau, I.-P., The defect chemistry of Ce(Pr, Zr)$O_{2-\delta}$. Journal of Solid State Chemistry, 179, No. 5, 1469-1477 (2006).

Fernandez-Garcia, M., Martinez-Arias, A., Iglesias-Juez, A., Hungria, A.-B., Conesa, J.-C., Soria, J., Structural characteristics and redox behavior of CeO_2–ZrO_2/Al_2O_3 supports. Journal of Catalysis, 194, No. 2, 385-392 (2000).

Fally, F., Perrichon, V., Vidal, H., Kaspar, J., Blanco, G., Pintado, J.-M., Bernal, S., Colon, G., Daturi, M., Lavalley, J.-C., Modification of the oxygen storage capacity of CeO2–ZrO2 mixed oxides after redox cycling aging. Catalysis Today, 59, No. 3-4, 373–386 (2000).

Fornasiero, P., Fonda, E., Di Monte, R., Vlaic, G., Kaspar, J., Graziani, M., Relationships between structural/textural properties and redox behavior in $Ce_{0.6}Zr_{0.4}O_2$ mixed oxides. Journal of Catalysis, 187, No. 1, 177-185 (1999).

Gonzalez-Velasco, J.-R., Gutierrez-Ortiz, M.-A., Marc, J.-L., Botas, J.-A., Gonzalez-Marcos, M.-P., Blanchard, G., TWC behavior of platinum supported on high and low surface area cerium sol zirconium mixed oxides. Topics in Catalysis, 16/17, No. 1-4, 101-106 (2001).

Guo, Y., Lu, G..-Z., Zhang, Z.-G., Zhang, S.-H., Qi, Y., Liu, Y., Preparation of $Ce_xZr_{1-x}O_2$ (X=0.75,0.62) solid solution and its application in Pd-only three-way catalysts. Catalysis Today, 126, No. 3-4, 296-302 (2007).

Hadi, A. and Yaacob, I.-I., Synthesis of PdO/CeO_2 mixed oxides catalyst for automotive exhaust emission control. Catalysis Today, 96, No. 3, 165-170 (2004).

He, H., Dai, H.-X., Wong, K.-W., Au, C.-T., $RE_{0.6}Zr_{0.4-x}Y_xO_2$ (RE = Ce, Pr; x = 0, 0.05) solid solutions: an investigation on defective structure,

oxygen mobility, oxygen storage capacity, and redox properties. Applied Catalysis A: General, 251, No. 1, 61-74 (2003).

Hickey, N., Fornasiero, P. Kaspar, J., Gatica, J.-M., Bernal, S., Effects of the nature of the reducing agent on the transient redox behavior of NM/$Ce_{0.68}Zr_{0.32}O_2$ (NM= Pt, Pd, and Rh). Journal of Catalysis, 200, No. 1, 181-193 (2001).

Hirohumi, S., Toshitaka, T., Hideo, S., Masahiro, S., Effect of Ba addition on catalytic activity of Pt and Rh catalysts loaded on γ-alumina, Topics in Catalysis, 16/17, No. 1-4, 95-99 (2001).

Jiang, P.-P., Lu, G.-Z., Guo, Y., Guo, Y.-L., Zhang, S.-H., Wang, X.-Y., Preparation and properties of a γ-Al_2O_3 washcoat deposited on a ceramic honeycomb. Surface & Coatings Technology, 190, No. 2-3, 314-320 (2005).

Kakuta, N., Ikawa, S., Eguchi, T., Murakami, K., Ohkita, H., Mizushima, T., Oxidation behavior of reduced $(CeO_2)_{1-x}$-$(ZrO_2)_x$ (x = 0, 0.2, 0.5) catalysts. Journal of Alloys and Compounds, 408-412, 1078-1083 (2006).

Kaspar, J. and Fornasiero, P., Nanostructured materials for advanced auto motive de-Pollution catalysts. Journal of Solid State Chemistry, 171, No. 1-2, 19-29 (2003).

Kaspar, J., Fornasiero, P., Balducci, G., Di Monte, R., Hickey, N., Sergo, V., Effect of ZrO_2 content on textural and structural properties of CeO_2-ZrO_2 solid solutions made by citrate complexation route. Inorganica Chimica Acta, 349, 217-226 (2003a).

Kaspar, J., Fornasiero, P., Hickey, N., Automotive catalytic converters: current status and some perspectives. Catalysis Today, 77, No. 4, 419-449 (2003b).

Kim, J.-R., Myeong, W.-J., Ihm, S.-K., Characteristics in oxygen storage capacity of ceria–zirconia mixed oxides prepared by continuous hydrothermal synthesis in supercritical water. Applied Catalysis B: Environmental, 71, No. 1-2, 57-63 (2007).

Kim, J.-R., Myeong, W.-J., Ihma, S.-K., Characteristics of CeO_2–ZrO_2 mixed oxide prepared by continuous hydrothermal synthesis in supercritical water as support of Rh catalyst for catalytic reduction of NO by CO. Journal of Catalysis, 263, No. 1, 123-133 (2009).

Kim, D.-H., Woo, S.-I., Yang, O.-B., Effect of pH in a sol–gel synthesis on the physicochemical properties of Pd–alumina three-way catalyst. Applied Catalysis B: Environmental, 26, No. 4, 285-289 (2000).

Kolli, T., Rahkamaa-Tolonen, K., Lassi, U., Savimaki, A., Keiski, R.-L., Comparison of catalytic activity and selectivity of Pd/(OSC + Al_2O_3) and (Pd + OSC)/Al_2O_3 catalysts. Catalysis Today, 100, No. 3-4, 297-302 (2005).

Kucharczyk, B., Tylus, W., Kepinski, L., Pd-based monolithic catalysts on metal supports for catalytic combustion of methane. Applied Catalysis B: Environmental, 49, No. 1, 27-37 (2004).

Lin, W., Zhu, Y.-X. Wu, N.-Z., Xie, Y.-C., Murwani, I., Kemnitz, E., Total oxidation of methane at low temperature over Pd/TiO_2/Al_2O_3: effects of the support and residual chlorine ions. Applied Catalysis B: Environmental, 50, No. 1, 59-66 (2004).

Luo, M.-F., Zheng, X.-M., Redox behavior and catalytic properties of $Ce_{0.5}Zr_{0.5}O_2$ supported palladium catalysts. Applied Catalysis A: General, 189, No. 1, 15-21 (1999).

Mokhnachuk, O.-V., Soloviev, S.-O., Kapran, A.-Yu., Effect of rare-earth element oxides (La_2O_3, Ce_2O_3) on the structural and physico-chemical characteristics of Pd/Al_2O_3 monolithic catalysts of nitrogen oxide reduction by methane. Catalysis Today, 119, No. 1-4, 145-151 (2007).

Monte, R.-D., Fornasiero, P., Kašpar, J, Rumori, P., Gubitosa, G., Pd/$Ce_{0.6}Zr_{0.4}O_2$/Al_2O_3 as advanced materials for three-way catalysts Part 1. Catalyst characterisation, thermal stability and catalytic activity in the reduction of NO by CO. Applied Catalysis B: Environmental, 24, No. 3-4, 157-167 (2000).

Montoya, J.-A., Romero-Passual, E., Gimon, C., Del Angel, P., Monzon, A., Methane reforming with CO_2 over Ni/ZrO_2-CeO_2 catalysts prepared by sol-gel. Catalysis Today, 63, No.1, 71-85 (2000).

Morikawa, A., Suzuki, T., Kanazawa, T., Kihiko, K., Suda, A., Shinjo, H., A new concept in high performance ceria–zirconia oxygen storage capacity material with Al_2O_3 as a diffusion barrier. Applied Catalysis B: Environmental, 78, No. 3-4, 210-221 (2008).

Morikawa, A., Kikuta, K., Suda, A., Shinjo, H., Enhancement of oxygen storage capacity by reductive treatment of Al_2O_3 and CeO_2–ZrO_2 solid solution nanocomposite. Applied Catalysis B: Environmental, 88, No. 3-4, 542-549 (2009).

Muraki, H. and Geng, Z., Design of advanced automotive exhaust catalysts. Catalysis Today, 63, No. 2-4, 337-345 (2000).

Otsuka-Yao-Matsuo, S., Izu, N., Omata, T., Ikeda, K., Thermodynamic behavior of various phases appearing in the $CeZrO_4$-$CeZrO_{3.5}$ system and the formation of metastable solid solutions. Journal of Electrochem. Society, 145, No. 4, 1406-1413 (1998).

Pan, Y.-L., Wen, Y.-Y., Chen, Y.-Q., Gong, M.-C., Effect of doping manganese on the properties of CeO_2-ZrO_2-Al_2O_3. Chemical Journal of Chinese Universities, 30, No. 2, 337-343 (2009).

Pawlak, D.-A., Lukasiewicz, T., Carpenter, M., Malinowski, M., Diduszko, R., Kisielewski, J., Czochralski crystal growth, microstructure and spectroscopic properties of $PrAlO_3$ perovskite. Journal of Crystal Growth, 282, No. 1-2, 260-269 (2005).

Perrichon, V., Laachir, A., Beregeret, G., Frety, R., Tournayan, L., Touret, O., Reduction of cerias with different textures by hydrogen and their reoxidation by oxygen. Journal of the Chemical Society Faraday Transactions, 90, No. 5, 773-781 (1994).

Piras, A., Trovarelli, A., Dolcetti, G., Remarkable stabilization of transition alumina operated by ceria under reducing and redox conditions. Applied Catalysis B: Environmental, 28, No. 2, L77-L81 (2000).

Salasc, S., Perrichon, V., Perrichon, M., Primet, M., Mouaddib-Moral, N., Titration by oxygen of the spill-over hydrogen adsorbed on ceria–zirconia supported palladium–rhodium catalysts. Journal of Catalysis, 206, No. 1, 82-90 (2002).

Silva, F.-A., Martinez, D.-S., Ruiz, J.-A.-C., Mattos, L.-V., Hori, C.-E., Noronha, F.-B., The effect of the use of cerium-doped alumina on the performance of $Pt/CeO_2/Al_2O_3$ and $Pt/CeZrO_2/Al_2O_3$ catalysts on the partial oxidation of methane. Applied Catalysis A: General, 335, No. 2, 145-152 (2008).

Stary, T., Solcova, O., Schneider, P., Marker, M., Effective diffusivities and pore-transport characteristics of washcoated ceramic monolith for automotive catalytic converter. Chemical Engineering Science, 61, No. 18, 5934-5943 (2006).

Suopankia, A., Polvinen, R., Valden, M., Harkonen, M., Rh oxide reducibility and catalytic activity of model Pt–Rh catalysts. Catalysis Today, 100, No. 3-4, 327-330 (2005).

Sun, K.-P., Lu, W.-W., Wang, M., Xu, X.-H., Characterization and catalytic performances of La doped Pd/CeO_2 catalysts for methanol decomposition. Applied Catalysis A: General, 268, No. 1-2, 107-113 (2004).

Thammachart, M., Meeyoo, V., Risksomboon, T., Osuwan, S., Catalytic activity of CeO_2–ZrO_2 mixed oxide catalysts prepared via sol–gel technique: CO oxidation. Catalysis Today, 68, No. 1-3, 53-61 (2001).

Tian, J.-Y., Lu, J.-S., Mu, L.-L., Du, B.-X., Study on the performance and preparation of $Ce_{0.6}Zr_{0.35}Pr_{0.05}O_2$ nano solid solution. Journal of Chinese Material Science Engineering, 24, No. 5, 730-732 (2006).

Tian, J.-Y., Lu, J.-S., Wu, H., Effect of additive polyethylene glycol on γ-Al_2O_3 washcoat properties of cordierite ceramic honeycomb. Journal of Chinese University Chemical Engineering, 24, No. 1, 167-170 (2010).

Vidal, H., Kaspar, J., Pijolar, M., Colon, G., Bernal, S., Cordon, A., Perrichon, V., Fally F., Redox behavior of CeO_2-ZrO_2 mixed oxides Influence of redox treatments on high surface area catalysts. Applied Catalysis B: Environmental, 27, No. 1, 49-63 (2000).

Wang, J.-O., Shen M.-Q., An, Y., Wang, J., Ce–Zr–Sr mixed oxide prepared by the reversed microemulsion method for improved Pd-only three-way catalysts. Catalysis Communications, 10, No. 1, 103-107 (2008).

Wang, G., Meng, M., Zha, Y.-Q., Ding, T., High-temperature close coupled catalysts Pd/Ce–Zr–M/Al2O3 (M = Y, Ca or Ba) used for the total oxidation of propane. Fuel, 89, No. 9, 2244-2251 (2010).

Wei, Z.-L, Li, H.-M, Zhang, X.-Y, Yan, S.-H, Lv, Z, Chen, Y. Q, Gong, M. C., Preparation and property investigation of CeO_2-ZrO_2-Al_2O_3 oxygen-storage compounds. Journal of Alloy and Compound, 455, No. 1-2, 322-326 (2008).

Wu, X.-D., Xu, L.-H., Weng, D., The thermal stability and catalytic performance of Ce-Zr promoted Rh-Pd/γ-Al_2O_3 automotive catalysts. Applied Surface Science, 221, No. 1-4, 375-383 (2004).

Wu, X.-D., Fan, J., Ran, R., Yang, J., Weng, D., Effect of preparation method on the surface and redox properties of $Ce_{0.67}Zr_{0.33}O_2$ mixed oxides. Journal of Alloy and Compounds, 395, No. 1-2, 135-140 (2005).

Wu, X.-D., Wu, X.-D., Liang, Q., Fan, J., Weng, D., Xie, Z., Wei, S.-Q., Structure and oxygen storage capacity of Pr/Nd doped CeO_2–ZrO_2 mixed oxides. Solid State Science, 9, No. 7, 636-643 (2007).

Al-Yassir, N., and Le Van Mao, R., Thermal stability of alumina aerogel doped with yttrium oxide, used as a catalyst support for the thermocatalytic cracking (TCC) process: an investigation of its textural and structural properties. Applied Catalysis A: General, 317, No. 2, 275-283 (2007).

Yao, H.-C., Yu Yao, Y.-F., Ceria in automotive exhaust catalysts: I. Oxygen storage. Journal of Catalysis, 86, No. 2, 254-265 (1984).

Yeste, M.-P., Hernandez, J.-C., Bernal, S., Blanco, G., Calvino, J.-J., Perez-Omil, J.-A., Pintado, J.-

M., Comparative study of the reducibility under H_2 and CO of two thermally aged $Ce_{0.62}Zr_{0.38}O_2$ mixed oxide samples. Catalysis Today 141, No. 3-4, 409-414 (2009).

Yue, B., Zhou, R., Wang, Y., Zheng, X., Effect of rare earths (La, Pr, Nd, Sm and Y) on the methane combustion over Pd/Ce-Zr/Al_2O_3 catalysts. Applied Catalysis A: General, 295, No. 1, 31-39 (2005).

Yue, B.-H., Zhou, R-X., Wang, Y.-J., Zheng, X.-M., Influence of transition metals (Cr, Mn, Fe, Co and Ni) on the methane combustion over Pd/Ce-Zr/Al_2O_3 catalyst. Applied Surface Science, 252, No. 16, 5820-5828 (2006).

Zhao, M., Chen, S.-H., Zhang, X.-Y., Gong, M.-C., Chen, Y.-Q., Performance of Pd/ CeO_2-ZrO_2 - Al_2O_3 catalyst for motorcycle. Journal of Rare Earths, 27, No. 5, 728-732 (2009).

Zhang, X.-Y., Long, E.-Y., Li, Y.-L., Guo, J.-X., Zhang, L.-J., Gong, M.-C., Wang, M.-H., Chen, Y.-Q., CeO_2-ZrO_2-La_2O_3-Al_2O_3 composite oxide and its supported palladium catalyst for the treatment of exhaust of natural gas engined vehicles. Journal of Natural Gas Chemistry, 18, No. 2, 139-144 (2009).

Zhu, L.-Y., Yu, G., Oin, W.-W., Wang, X.-Q., Xu, D., Preparation, morphology and specific surface area of CeO_2-ZrO_2 and CeO_2-ZrO_2-Al_2O_3 fine fibers via precursor sol-gel technique. Journal of Alloys and Compound, 492, No. 1-2, 456-460 (2010).

Zhu, Z., Wan, C.-Z., Lui, Y.-K., Dettling, J., Steger, J.-J., Design of a novel Pd three-way catalyst: integration of catalytic function in three dimensions. Catalysis Today, 30, No. 1-3, 83-89 (1996).

Zotin, F.-M.-Z., Gomes, O.-F.-M., Cristiano, O., Neto, A.-A., Cardoso, M.-J.-B., Automotive catalyst deactivation: case studies. Catalysis Today, 107-108, 157-167 (2005).